Biochimica et Biophysica Acta, 1102 (1992) 67–75

BBABIO 43645

Theoretical studies on the control of the oxidative phosphorylation system

Bernard Korzeniewski and Wojciech Froncisz

Institute of Molecular Biology, Jagiellonian University, Kraków (Poland)

(Received 17 December 1991)
(Revised manuscript received 31 March 1992)

Key words: Theoretical study; Oxidative phosphorylation; Metabolic control theory; Computer simulation

The dynamic model developed in our previous publications [1,2] was used to calculate the flux control coefficients of oxidation, phosphorylation and proton leak fluxes for isolated mitochondria and for three modes of work of intact cells (hepatocytes). The results obtained were compared with experimental data, especially those measured in the frame of the 'top-down approach' of the metabolic control theory. A good agreement for mitochondria and for intact cells was found. The control of the oxygen consumption flux is shared between the ATP utiiization (main controlling factor), substrate dehydrogenation, proton leak and, in some conditions, the ATP/ADP carrier. The phosphorylation subsystem seemed to be controlled mainly by itself, while the proton leak was influenced by all three subsystems. It was also shown that the large relative change in the enzyme activity during inhibitor titration of mitochondria or cells could lead to the overestimation of some flux control coefficient values in experimental measurements. An influence of some hormones (glucagon, vasopressin, adrenaline and others) on the mitochondrial respiration was also simulated. Our results suggest that these hormones stimulate the substrate dehydrogenation as well as the phosphorylation system (ATP usage and, possibly, the ATP/ADP carrier).

Introduction

The best means of describing the extent of enzyme (or process) control of the flux through a given metabolic pathway is the metabolic control theory [3–6]. According to this theory none of the enzymes uniquely determines the flux through a pathway. The participation of each enzyme in the control of a flux is described by a parameter called the 'flux control coefficient' (fcc). It is defined as the ratio of the relative change in a given flux caused by the small relative change in the enzyme concentration (activity) to the change itself. If we deal with the influence of an enzyme i on flux m then the adequate fcc is equal to:

$$C_{E_i}^{J_m} = (\delta J_m / J_m)/(\delta E_i / E_i), \quad (1)$$

where J indicates flux and E indicates enzyme concentration (activity). The flux control coefficient is a global parameter – it depends on the properties of a whole system, not only on the features of a given enzyme, depending also on system conditions. So, any comparison should be performed for similar conditions. Moreover, during experimental measurements, the conditions should be established as close to physiological conditions as possible if physiological relevance is desired. The sum of fcc values of all enzymes (processes) in relation to a given flux is always equal to 1 – it is the co-called 'summation property'.

The parameter which determines the influence of a given metabolite on the activity of a given enzyme is an elasticity coefficient. It is defined as the relative change in enzyme activity divided by the small relative change

Correspondence to: B. Korzeniewski, Institute of Molecular Biology, Jagiellonian University, Kraków, Poland.

In all equations, concentrations of chemical compounds are represented by symbols written without square brackets for clarity and simplicity.

Abbreviations: a_r, a relative affinity of ATP to the ATP/ADP carrier with respect to ADP; fcc, flux control coefficient; k_x, k_{bx}, forward and backward rate constant of reaction x; K_x, equilibrium constant of reaction x; K_{Mx}, Michaelis-Menten constant of reaction x; N, concentration of the oxidized form of NAD; Nh, concentration of the reduced form of NAD; R_{cm}, ratio of cell to mitochondria volume; TCA cycle, tricarboxylic acid cycle; (subscripts) DEHY (D), substrate dehydrogenation; CONS (C), internal ATP consumption; UTIL (U), external ATP utilization; GLYC (G), glycolysis; 'e', external; 'i', internal; 'f', free; 'm', magnesium complex; 't', total.

in a metabolite concentration. The elasticity coefficient for metabolite n and enzyme i is:

$$\varepsilon^{i}_{S_n} = (\delta v_i / v_i)/(\delta S_n / S_n), \quad (2)$$

where v indicates reaction rate and S indicates metabolite concentration. The elasticity coefficient is a local parameter – it is a property of a particular enzyme under conditions where all other metabolite concentrations are kept constant.

An inhibitor titration is usually used for measuring the flux control coefficients in experiments. After addition of a small amount of the inhibitor, specific for a given enzyme, the initial decrease in a flux intensity is measured. Nevertheless, the relative changes used are often high, even equal to 0.25 of the initial enzyme activity [7].

The metabolic control theory is widely applied in the oxidative phosphorylation system. A number of experiments have been performed which have dealt with the measurements of the flux control coefficients for different enzymes (processes) in isolated mitochondria and intact cells, with respect to the oxygen consumption flux [7–14]. It is generally accepted that in physiological or quasi-physiological conditions (the substrate dehydrogenation and external ATP utilization present, state $3_{1/2}$) the control is shared between the ATP utilization, proton leak and, in some conditions, substrate dehydrogenation, cytochrome oxidase and the ATP/ADP carrier. The problem of the extent of control by the ATP/ADP carrier is most controversial. Groen et al. in mitochondria [7] and Duszyński et al. [10] as well as Tager et al. [11] in hepatocytes obtained values near 0.2–0.3 in the state $3_{1/2}$. On the other hand, practically no control was stated in other experiments with isolated mitochondria [8,9,15,16]. Moreover, some measurements [10,11] were performed under gluconeogenesis conditions, which differ markedly from a mitochondrial hexokinase system and an intact hepatocytes resting state. Thus this problem seems to be unsolved entirely till now.

A new tool for researching the control over the oxidative phosphorylation system arose with a 'top-down approach' to the metabolic control theory [18–20]. It enables us to fix the flux control coefficients of whole subsystems instead of particular enzymes. In the publications mentioned flux control coefficients of the oxidation, phosphorylation and proton leak subsystems over the oxidation, phosphorylation and proton leak fluxes were calculated. The oxidation subsystem consists of the substrate dehydrogenation, respiratory chain and cytochrome oxidase; the phosphorylation subsystem contains ATP synthetase, ATP/ADP carrier, phosphate carrier, adenylate kinase, internal and external ATP usage; the proton leak subsystem includes only the proton leak. The calculation was based on the relative values of the three fluxes and on the values of elasticity of those subsystems on a 'central intermediate' – the protonmotive force $\Delta\mu_{H^+}$. An assumption that the subsystems influence each other only by this intermediate was the condition of the validity of the calculations. The results obtained were rather similar for isolated mitochondria and intact hepatocytes. The oxidation flux was controlled by all three subsystems (with a domination of the phosphorylation one), while the phosphorylation system was regulated mostly by itself.

Up to now the flux control coefficients have not been measured for the different physiological states of cells. The factors distorting the obtained values of fcc values have not been assessed quantitatively. The purpose of our work is to compare calculated flux control coefficients with experimental results and to obtain theoretically the parameter values not measured till now. Of course, because of complexity of the simulated system, the results obtained can be considered as only semi-quantitative ones.

It has been uncertain until now which parts of the mitochondrial phosphorylation system are affected (probably through cAMP or Ca^{2+}) by hormones stimulating gluconeogenesis and ureogenesis (glucagon, vasopressin, adrenalin and others). Brand and Murphy in their extensive review [6] came to the conclusion that the main point of the action of these hormones is the substrate dehydrogenation (Ca^{2+}-dependent TCA cycle dehydrogenases). Having the verified model (at least semi-quantitatively) our purpose was to check this supposition.

Model

For the numerical simulations a dynamic model of the oxidative phosphorylation process developed in our previous publications [1,2] is used. Some modifications are named below.

First of all the description of the substrate dehydrogenation is changed. The one used in Ref. 2 is oversimplified (a linear dependence on $[NAD^+]$). It does not allow stimulation of the substrate dehydrogenation by an increase in NAD^+ concentration; the moiety-conservation property and the highly oxidized NAD pool determine that this process is almost saturated with NAD^+. So, an increased ATP usage would cause almost no effect on the respiratory rate (particularly if the substrate dehydrogenation dependence on the [ADP]/[ATP] ratio is considered to be weak). The substrate dehydrogenation would not be able to be activated by an increase in the acetyl-CoA concentration either, as the citrate synthetase is insensitive to it in a wide range [17]. In the present publication, we intended to reflect the properties of the tricarboxylate acids cycle. According to Williamson et al. [17], the

main controlling component of this cycle is the isocitrate dehydrogenase. This enzyme influences two other irreversible ones, namely the citrate synthetase and 2-oxoglutarate dehydrogenase, via the concentration of citrate and 2-oxoglutarate, respectively. The isocitrate dehydrogenase is effectively inhibited by NADH. The K_i constant is equal to about 16 μM [17] (about 0.05 μM in suspension). The apparent K_m constant for NAD^+ can be assessed for the physiological isocitrate concentration as equal to about 300 μM (0.88 μM in suspension). Taking into account the above mentioned facts we described the substrate dehydrogenation process by an equation, being a simple modification of the expression for the competitive inhibition:

$$v_{DEHY} = V_{maxD}/(1 + K_{MN}(1 + Nh/K_i)^m/N) \quad (3)$$

The power parameter m was adjusted to be equal to 0.45. This value is less than unity because of partial compensation of changes in the NAD pool redox level by changes in the concentration of citrate (and isocitrate). It must be emphasized that the presented description of the substrate dehydrogenation process is phenomenological and intuitive. In order to ensure its physiological relevance, adjusting the value of m, we checked its ability to imitate the inhibitor titration curves from Fig. 4 and 5 in Ref. 19 (a quite broad range of cell conditions). A good, at least semi-quantitative, agreement was finally stated. Thus, we assume that this description is a sufficient, phenomenological approximation. Of course, an adequate detailed model of the Krebs cycle would be better than a single, phenomenological equation and we plan to develop it in the future.

The value of the constant k_{L2} in the expression for the proton leak [2] is slightly enlarged from $9.0 \cdot 10^{-2}$ to $9.2 \cdot 10^{-2}$ mV^{-1} in order to obtain a slightly better agreement with the experiments.

Some minor changes were introduced to be in line with recent knowledge. We assume that complex I pumps four protons per two passing electrons. The cytochrome c mid-point redox potential value, equal to 260 mV, was accepted. The initial ΔpH value was slightly decreased to 36 mV. The resultant $[NAD^+]/[NADH]$ ratio was then equal to about 10. These changes did not significantly influence the properties of the model.

In order to reveal the pattern of the control over the respiration process under different cell conditions, we distinguished three modes of the work of cells (especially hepatocytes):

Mode 1, no additional ATP supply (glycolysis), β-oxidation of fatty acids as the source of reducing equivalents, fatty acids as a respiratory substrate, an external ATP utilization slightly dependent on the [ATP]/[ADP] ratio. This mode is similar to the conditions applied previously [2]. A kinetics of both external and internal ATP utilization is slightly changed (a dependence on the [ATP]/[ADP] ratio is applied):

$$v_{UTIL} = v_{maxU}/(1 + K_{MU}/(ATP_{te}/ADP_{te})) \quad (4)$$

$$v_{CONS} = v_{maxC}/(1 + K_{MC}/(ATP_{ti}/ADP_{ti})), \quad (5)$$

where $K_{MU} = 3$ and $K_{MC} = 0.5$.

Mode 2, glycolysis as a source of reducing equivalents and additional ATP supply, glucose as a respiratory substrate, the external ATP utilization weakly dependent on the [ATP]/[ADP] ratio. A differential equation describing the additional ATP supply by the glycolysis process is added to the original model. A linear dependence of this process on the [ADP]/[ATP] ratio is assumed. Of course such an assumption is only a rough approximation. An adequate expression is:

$$v_{GLYC} = k_g \times ADP_{te}/ATP_{te} \quad (6)$$

The rate constant k_g is calculated under the assumption that the ATP supply by the glycolysis is equal to about 10% of that by the oxidative phosphorylation in aerobiosis conditions, as assessed from relative fluxes of glycolytic and oxidative ATP synthesis. An influence of the glycolysis on the substrate dehydrogenation is neglected as it is assumed that the latter process is mainly controlled by Krebs cycle dehydrogenases (the flux through this cycle is independent on the pyruvate concentration over a wide range [17]). Hence, the only kinetic relationship between the glycolysis and phosphorylation systems occurs through a competition for ADP (Pasteur and Crabtree effect).

Mode 3, no additional ATP supply, lactate as a respiratory substrate, gluconeogenesis as a major ATP-utilizing reaction, strongly dependent on the [ATP]/[ADP] ratio. In comparison with the Mode 1, the additional external ATP utilization is introduced. This process is described by the equation analogous to Eqn. 4. The adequate Michaelis-Menten constant is increased 30-times (a near-linear dependence), while the maximal velocity is enlarged 7-times to increase the respiratory rate by about 30%. The mode of stimulated ureogenesis is not distinguished, as we assume that it is kinetically comparable with Mode 3.

The model for isolated mitochondria suspension is similar to that described in Ref. 2. Comparing with the cell Mode 1, the following changes are introduced: (1) a lack of cell volume – concentrations of the external ATP, ADP, AMP and P_i are determined in a suspension volume; (2) an external concentration of inorganic phosphate is 10 mM and of the adenine nucleotides pool is 1 mM, in agreement with experimental conditions [7,8]; concentrations of particular nucleotides were adjusted to obtain an external and internal phosphorylation potential comparable with that in intact cells,

maintaining the same displacement from equilibrium of the adenine nucleotide carrier and phosphate carrier; (3) only two coupling sites are considered (complex III and IV), since succinate is used as a substrate; a mid-point redox potential for a pool of reducing equivalents (succinate/fumarate, UQ, complex II), being near equilibrium, is assumed as equal to 0.00 mV; an oxygen consumption rate is assumed to be equal to 1.7 μM O_2 per s to maintain the phosphorylation rate at the same level; (4) the external ATP consumption is described as [ATP]-dependent, with Michaelis-Menten constant equal to 150 μM; (5) because of the near-linear relationship between $[ATP_{te}]/[ADP_{te}][P_{i_{te}}]$ and $(\Delta\mu_H/Z)^{n/4+1}$ is found in the simulation, the cytochrome oxidase is described as depending on the protonmotive force instead of on the external phosphorylation potential.

For calculation of the flux control coefficients, a dynamic property of the model is applied. The relative change of 0.001 in enzyme activity at the steady state of the system is performed. Then, when the system is stabilized, after a sudden change in the enzyme activity, it is possible to calculate the flux control coefficient for this enzyme.

The set of differential equations described in Ref. 2, and modified as mentioned above, is integrated using the Gear subroutine, designed especially for 'stiff' problems. Calculation programs are written in Microsoft Fortran. The simulations were performed using a PC/386 (33 MHz) computer, equipped with a coprocessor.

Results and Discussion

The simulated flux control coefficients of an oxygen consumption flux of main enzymes (processes) taking part in the oxidative phosphorylation are shown in Table I. Those for isolated mitochondria are similar to those calculated previously [2] in the framework of a slightly simpler model. Thus, a comparison with experimental results and a general discussion remain essentially the same. All simulated fcc values are in good agreement with the experiments. The only partial exception is a flux control coefficient for the adenine nucleotide carrier. This contradiction was discussed in Ref. 2 and will, additionally, be analyzed below. The fcc values for intact cells are rather similar to those for isolated mitochondria. Cells working in Mode 1 or Mode 2 are in the 'resting' state. This means that there is a low ATP utilization. ATP is consumed by reactions essential for the survival of a cell, for example a protein synthesis, an ion and substrate transport. They are 'base' reactions. In these conditions the ATP utilization is essentially independent on the [ATP]/[ADP] ratio [21]. In Mode 3 the main ATP-utilizing reaction is gluconeogenesis. Its substrate, lactate (or others, being relatively near the equilibrium with lactate, for example, pyruvate or dihydroxyacetone), which is in excess, causes an inhibition of the glycolysis and β-oxidation, and an adequate activation of the gluconeogenesis, and hence, ATP utilization. The gluconeogenesis is much more sensitive to the [ATP]/[ADP] ratio than 'base' reactions. This is obvious, because, at a lower phosphorylation potential, all reactions not needed immediately for keeping the cell alive must be 'turned off'. Thus Mode 3 represents an 'active' state of a cell. If we pass from isolated mitochondria via the 'resting' state of a cell to the 'active' one, we can see a gradual, directional change in the fcc values for some processes. While the fcc value for the ATP utilization exhibits a clear decrease, the fcc values for the substrate dehydrogenation and ATP/ADP carrier increase. Stated simply, in a less 'restricted' energetic state, the ATP utilization is allowed to relax the control over respiration – the increased rate of the oxidative phosphorylation is able to meet the demand for the ATP of 'base' reactions and gluconeogenesis. Under these conditions the control can be shifted to the substrate dehydrogenation and the ATP/ADP carrier. Among the fcc values mentioned for cell conditions, only this one for the ATP/ADP carrier has been measured experimentally [10,11]. The value obtained was 0.25–

TABLE I

Simulated flux control coefficients of the oxygen consumption flux in isolated mitochondria and intact cells

Enzyme (reaction)	Mitochondria	Cells		
		Mode 1	Mode 2	Mode 3
Substrate dehydrogenation	0.09	0.14	0.14	0.36
Cytochrome oxidase	0.09	0.04	0.05	0.06
ATP synthetase	0.00	0.00	0.00	0.00
Internal ATP consumption	0.02	0.02	0.02	0.01
ATP/ADP carrier	0.02	0.13	0.17	0.22
Phosphate carrier	0.00	0.01	0.02	0.02
External ATP utilization	0.59	0.48	0.46	0.24
Glycolysis	–	–	−0.05	–
Proton leak	0.19	0.18	0.19	0.09

0.28. Nevertheless, it must be emphasized that both studies mentioned were performed in the Mode 3 conditions. Thus, they are in good agreement with our theoretical results (some difference can be caused, for example, by an overestimation of flux control coefficient values using a graphic method – see below). However, this value cannot be extrapolated, either to the other modes in cells, or to mitochondria. The higher fcc value for the ATP/ADP carrier in state 2 than in state 1 is in line with the conclusion based on experimental results [8,9] that the additional ATP supply enhances the control of this enzyme. However, the increase in the strength of the control is smaller than in cited publications because the ATP influx from the glycolysis is much smaller than the one from the pyruvate kinase used in these experiments.

Generally, we obtained results indicating that both in mitochondria and in cells the control of the oxygen consumption flux is distributed between the ATP utilization, proton leak and, under some conditions, substrate dehydrogenation and the ATP/ADP carrier.

In Table II a comparison is made between the 'top-down approach' to the metabolic control theory [20] and simulations based on our model for mitochondria conditions. A fairly good agreement can be stated, supporting validity of the model. On the other hand, experimental conditions are better defined in mitochondria than in cells. For example, because of applying succinate as a substrate, there is no danger that the phosphorylation system can affect the oxidative system differently than by Δp (key dehydrogenases of the tricarboxylate cycle are sensitive to the [ADP]/[ATP] ratio).

Table III shows the flux control coefficient values of the three distinct subsystems in the cells working in Mode 1. The comparison between experimental [19]

TABLE II

Simulated flux control coefficients of oxidation, phosphorylation and proton leak subpathways of oxidation, phosphorylation and proton leak fluxes in isolated mitochondria compared with experimental results obtained in the frame of the 'top-down approach' of metabolic control theory [a]

Subpathway	Oxidation flux	Phosphorylation flux	Proton leak flux
Oxidation			
simulated	0.18	0.01	0.77
experimental	≈ 0.15	≈ 0.00	≈ 0.60
Phosphorylation			
simulated	0.63	0.99	−0.60
experimental	≈ 0.65	≈ 1.00	≈ −0.50
Proton leak			
simulated	0.19	0.00	0.83
experimental	≈ 0.20	≈ 0.00	≈ 0.90

[a] See Ref. 20.

TABLE III

Simulated flux control coefficients of oxidation, phosphorylation and proton leak subpathways of oxidation, phosphorylation and proton leak fluxes in intact hepatocytes working in the Mode 1 compared with experimental results obtained in the frame of the 'top-down approach' of metabolic control theory for starved rats [a]

Subpathway	Oxidation flux	Phosphorylation flux	Proton leak flux
Oxidation			
simulated	0.18	0.09	0.54
experimental	0.27	0.21	0.48
Phosphorylation			
simulated	0.64	0.93	−0.42
experimental	0.57	0.84	−0.37
Proton leak			
simulated	0.18	−0.02	0.88
experimental	0.16	−0.05	0.89

[a] See Ref. 19.

(starved rats) and simulated results exhibits a good agreement for most fcc values. The main differences are in the control of the oxidation and phosphorylation fluxes by the oxidation subsystem. To explain these differences, we have calculated the elasticity coefficients for all three subsystems with respect to Δp and compared them with the experimentally measured ones. It is important to know their values because they serve together with the relative flux intensities to calculate the fcc values in the context of the 'top-down approach'. We obtained for the oxidation, phosphorylation and proton leak flux: −6.46 (−6.1), 0.66 (1.7) and 4.22 (4.0), respectively (experimental values in brackets). Thus, the simulated elasticities of the oxidation and the proton leak subsystems agree well with the experimental ones. On the contrary, the simulated elasticity for the phosphorylation system is almost 3-times smaller than the experimental one. Of course, the first reason for this disagreement can be the invalidity of the model, especially kinetics of the ATP utilization. Nevertheless, we simulated the elasticity for the case where the ATP utilization was linearly dependent on the [ATP]/[ADP] [P_i] ratio (a very strong dependence) and we obtained a value of 1.36, which was still smaller than the measured one. In fact, a much smaller dependence of the 'base' reactions on the phosphorylation potential should be expected. On the other hand, we used in our simulations a 'nearly-infinitesimal' relative change in the oxidation system activity (0.001), while Brown et al. [19], during myxothiazol titration, applied a change, which lowered the respiratory rate by about 20% (Fig. 5 in the cited paper). When we had introduced such a change, we obtained the elasticity coefficient value for the phosphorylation subsystem with respect to the proton-motive force equal to 1.67, which is very similar to the

TABLE IV

Simulated flux control coefficients of oxidation, phosphorylation and proton leak subpathways of oxidation, phosphorylation and proton leak fluxes in intact hepatocytes working in the Mode 2, compared with experimental results obtained in the frame of the 'top-down approach' of metabolic control theory for red rats [a]

Subpathway	Oxidation flux	Phosphorylation flux	Proton leak flux
Oxidation			
simulated	0.19	0.10	0.52
experimental	0.29	0.23	0.42
Phosphorylation			
simulated	0.62	0.93	−0.40
experimental	0.49	0.84	−0.29
Proton leak			
simulated	0.19	−0.02	0.88
experimental	0.22	−0.07	0.87

[a] See Ref. 19.

experimental one. Thus, we can state that the obtained experimental value is not a 'real' coefficient, but only a 'large-scale' one. This discrepancy has, thus, been successfully clarified. It indicates how important it is to apply as little relative change in an enzyme activity as possible during inhibitor titrations.

Table IV presents a comparison of the fcc values obtained experimentally for a suspension of cells isolated from fed rats [19] and simulated for Mode 2. The results are rather similar to those in Table III. Thus, the discussion made for Mode 1 remains valid for Mode 2. Taking it into consideration, a good agreement with experimental results can be stated.

Table V shows the fcc value simulated for Mode 3. Generally, the pattern of control is similar to the two other modes. Nevertheless, passing from the mitochondrial conditions through Modes 1 and 2 to Mode 3, a clear increase of the fcc values for the oxidation system, and a decrease of the fcc values for the phosphorylation system, can be stated. It is due to the release of the control of the phosphorylation system in the 'active' state.

Our theoretical results, which are in semi-quantitative agreement with the experimental ones [19,20], show that the oxidation flux is controlled by all three subsystems, with the greatest fcc value being for the phosphorylation subsystem. The latter is controlled mostly by itself, so it is only weakly influenced by the two others (the only exception being Mode 3). The large fcc value of the oxidation subsystem over the proton leak flux suggests that the proton leak acts as a 'buffer' for changes in the oxidation flux, maintaining the phosphorylation flux essentially unchanged. This conclusion is very important for the discussion on the stimulation of the oxidative phosphorylation system by hormones (see below).

In our previous publication [2], we discuss the relatively high value of the flux control coefficient for ATP/ADP carrier in a mitochondrial hexokinase system in the state $3_{1/2}$, measured by Groen et al. [7]. Here we intend to extend this discussion. Gellerich et al. [8], who obtained practically no control for the ATP/ADP carrier in the conditions mentioned, suggest that the reason is the great relative change (25%) in the carrier activity during carboxyatractyloside titration described in Ref. 7. In order to assess this supposition quantitatively, we simulated the dependence of the flux control coefficient for the carrier considered on the relative change in the carrier activity (or concentration). The results are presented in Table VI. It can be seen that, for the relative change used by Groen et al. [7], the measured fcc value can be overestimated by as much as 2-times. The second reason can be a slow return of the system to equilibrium, although rather fast transitions have been measured experimentally [22]. Further, as is shown by Gellerich et al. [23], the graphic method of the fixing of the flux control coefficients leads to the overestimation of the real value. And, finally, we stated in our model that the fcc value for the ATP/ADP carrier is essentially dependent on the external magnesium concentration. An analysis of the kinetic model of this carrier proposed by

TABLE V

Simulated flux control coefficients of oxidation, phosphorylation and proton leak subpathways of oxidation, phosphorylation and proton leak fluxes in intact hepatocytes working in the Mode 3

Subpathway	Oxidation flux	Phosphorylation flux	Proton leak flux
Oxidation			
simulated	0.42	0.39	0.63
Phosphorylation			
simulated	0.49	0.67	−0.53
Proton leak			
simulated	0.09	−0.06	0.90

TABLE VI

Simulated flux control coefficients of ATP/ADP carrier of oxygen consumption flux in isolated mitochondria at different relative changes in the carrier activity

Relative change in carrier activity	FCC [a]	MRV [b]
≈ 0.00	0.0248	1.00
0.125	0.0332	1.33
0.25	0.0480	1.93
0.5	0.1470	5.90

[a] Flux control coefficient.
[b] Multiplication of the real value.

us [2] reveals that the changes in the $[ADP_{fe}]/([ADP_{fe}] + a_r \times [ATP_{fe}])$ ratio are responsible for more than 85% of the changes in the overall carrier activity. This ratio is influenced by the external magnesium concentration. The latter parameter is fixed differently in different experiments and has commonly a higher value than in intact cells. It can cause the obtained fcc values for the ATP/ADP carrier to not be entirely relevant physiologically.

It has been shown that hormones such as glucagon, vasopressin and others, stimulate the gluconeogenesis and ureogenesis, as well as the respiration [6,24–27]. The basic question is which parts of the whole oxidative phosphorylation system are activated by these hormones. Brand and Murphy [6], discussing some possibilities, draw the conclusion that the main stimulated point is the substrate dehydrogenation process (Ca^{2+}-sensitive TCA cycle dehydrogenases). This opinion is supported in Ref. 19. However, results obtained in this paper suggest that the phosphorylation system (and, hence, gluconeogenesis and ureagenesis) can be stimulated by the increase in the oxidation flux intensity only slightly, the rest of this increase being 'buffered' by the proton leak. The fact that an increase in the level of the NAD and cytochrome *c* reduction [25], as well as in the internal [ATP]/[ADP] ratio [27], can be observed after the hormone addition, does not necessarily lead to the conclusion that the substrate dehydrogenation system is activated mainly or uniquely, but proves only that this system is stimulated as well. The experimental findings that, after the hormone addition, the protonmotive force, remains essentially unchanged [26], suggest that the stimulation of the phosphorylation system is of the same order of magnitude. To support these intuitive considerations, we simulated the hormone influence on the oxidative phosphorylation system in two models. In Model A only the substrate dehydrogenation is stimulated while in Model B the phosphorylation system is activated with hormones as well. The simulations for both models are divided into three stages, the first two being the same. Stage 1 is Mode 1 of the cell work. Stage 2 begins after the lactate addition and, hence, is comparable with Mode 3. In Stage 3, hormone-caused stimulation occurs. The relative respiratory rates of the particular stages are from Ref. 24 and amount to approx. 100%, 130% and 180%, respectively. In Stage 2 the additional external ATP utilization (corresponding to the gluconeogenesis) is described by the equation analogous to Eqn. (4), with the constants $V_{maxU2} = 7 \cdot V_{maxU}$ and $K_{MU2} = 20 \cdot K_{MU}$. In Stage 3 of Model A, the maximal velocity for the substrate dehydrogenation V_{maxD} is increased 10-times and K_{mN} is decreased 20-times. Stage 3 of Model B is characterized by the following changes: the substrate dehydrogenation and the phosphorylation system, apart from the ATP utilization, is activated 2-times, $K_{MU2} = K_{MU} = 0.25 \cdot K_{MU}$ from Stages 1 and 2, $V_{maxU2} = 0.9 \cdot V_{maxU}$. The results obtained are presented in Figs. 1 and 2 and in Table VII. Fig. 1 shows the three stages of Model A. It can be clearly seen that stimulation solely of the substrate dehydrogenation causes only a weak increase in the phosphorylation flux, the rest of the activation being 'buffered' by the proton leak. A quite different situation occurs in the Fig. 2, reflecting Model B. There, practically all the enhancement of the oxidation system is utilized by the increased activity of the phosphorylation system, the proton leak remaining essentially unchanged. Thus,

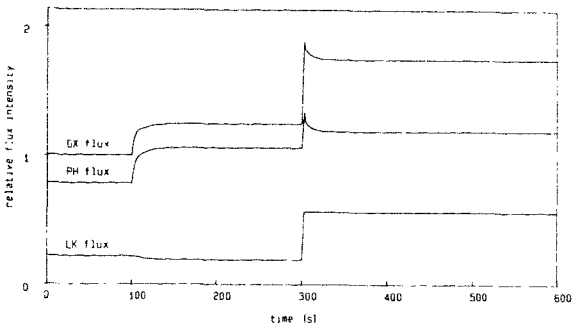

Fig. 1. The relative intensities of three fluxes before and after hormone action in Model A. After 100 s lactate is added, after 300 s hormone is introduced. OX flux, oxidation flux; PH flux, phosphorylation flux; LK flux, proton leak flux.

TABLE VII

Comparison between two models of hormone action on oxidative phosphorylation system

Model A, only substrate dehydrogenation stimulated and Model B, phosphorylation system activated as well.

Metabolic state	Cyt. *c* reduction (%)	NAD reduction (%)	$\Delta\tilde{\mu}_{H^+}$ (mV)	$[ATP_i]/[ADP_i]$	FCC (exch.)
Resting state	18.3	8.45	181.0	1.77	0.13
Lactate added	15.7	1.18	174.3	0.99	0.22
Hormone added					
model A	24.7	99.1	206.6	18.2	0.25
model B	30.2	12.6	177.5	1.29	0.05

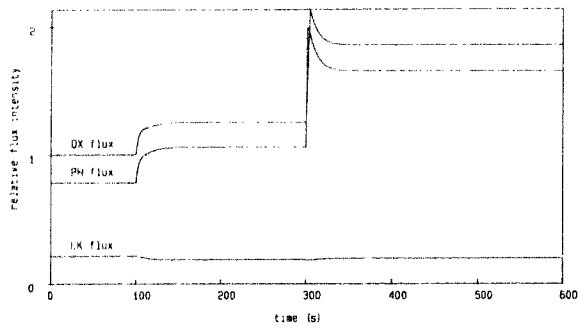

Fig. 2. The relative intensities of three fluxes before and after hormone action in Model B. After 100 s lactate is added, after 300 s hormone is introduced. OX flux, oxidation flux; PH flux, phosphorylation flux; LK flux, proton leak flux.

Model B reflects the experimental results much better. It must be emphasized that the oxidation flux, being the sum of the two others, changes similarly in both models. Further comparison is given in Table VII. Chosen parameter values of the common Stages 1 and 2 and of Stage 3 of both models are presented there. It can be seen that the hormone addition in Model A leads to the enormous increase in the level of NAD reduction, protonmotive force, internal [ATP]/[ADP] ratio and fcc value for ATP/ADP carrier, none of them being confirmed by experiments [24–27]. On the other hand, Model B agrees with the experiments very well (of course only a semi-quantitative comparison is possible). This model shows that, after the hormone addition, there is some increase in the NAD and cytochrome *c* reduction level [25], a moderate increase in the internal [ATP]/[ADP] ratio [27], and an essentially constant protonmotive force [26]. In spite of this, the calculated flux control coefficients of the ATP/ADP carrier in Stages 2 and 3 agree well with the experimental findings of Tager et al. [11]. These authors measured the fcc value of this carrier as equal to 0.26–0.28 in Mode 3, this value reducing to nearly zero after the glucagon addition. Our simulations are in line with the authors' conclusion that this hormone changed the ATP-utilizing system's elasticity with respect to the external [ATP]/[ADP] ratio. We must emphasize that such good agreement with experimental measurements is difficult to obtain for any realistic conditions without stimulation of the ATP/ADP carrier. So, our conclusion is that the hormones mentioned influence the substrate dehydrogenation as well as the phosphorylation system (external ATP utilization and, possibly, ATP/ADP carrier). It must be emphasized that the simulations described above are performed for Mode 3 (gluconeogenesis present). Hormone addition to the resting cells' suspension would yield a somewhat different result, as there is no gluconeogenesis to be stimulated. The adequate description for such conditions would be probably intermediate between Model A and B (maybe closer to Model A). However, such a situation seems to occur rather seldomly in intact living organisms. We do not claim that our model has finally resolved the problem discussed, but we believe it supplies a strong hypothesis.

The content of the presented work is the theoretical treatise of the problem of the mechanism controlling of the oxidative phosphorylation system. The dynamic model described in our previous paper is verified by a comparison with experimental results and then used to obtain some new information about the system. Because of its complexity, the results obtained can often only be compared with experiments semiquantitatively. Taking into account this limitation, the model reflects the properties of the system well and is a useful tool for researching the problems that have not been entirely resolved in an experimental way up till now. Of course, subsequent verification will be necessary.

References

1 Korzeniewski, B. and Froncisz, W. (1989) Studia Biophys. 132, 173–187.
2 Korzeniewski, B. and Froncisz, W. (1991) Biochim. Biophys. Acta 1060, 210–223.
3 Kacser, H. and Burns, J. (1973) Symp. Soc. Exp. Biol. 27, 65–107.
4 Heinrich, R. and Rapoport, T.A. (1974) Eur. J. Biol. 42, 107–120.
5 Kacser, H. and Porteous, J.W. (1987) Trends Biochem. Soc. 12, 5–14.
6 Brand, M.D. and Murphy, M.P. (1987) Biol. Rev. 62, 141–193.
7 Groen, A.K., Wanders, R.J.A., Westerhoff, A.W., Van der Meer, R. and Tager, J.M. (1982) J. Biol. Chem. 257 (6), 2754–2757.
8 Gellerich, F.N., Bohnensack, R. and Kunz, W. (1983) Biochim. Biophys. Acta 722, 381–391.
9 Bohnensack, R., Gellerich, F.N., Schild, L. and Kunz, W. (1990), Biochim. Biophys. Acta 1018, 182–184.
10 Dyszyński, J., Groen, A.K., Wanders, R.J.A., Vervoorn, R.C. and Tager, J.M. (1982) FEBS Lett. 146 (2), 262–266.
11 Tager, J.M., Groen, A.K., Wanders, R.J.A., Duszyński, J., Westerhoff, H.W. and Vervoorn, R.C. (1983) in Isolation, Characterization and Use of Hepatocytes, ed. (Harris, R.A. and Cornell, N.W., eds.), pp. 313–322, Elsevier, Amsterdam.
12 Doussiere, J., Ligeti, E., Brandolin, G. and Vignais, P.V. (1984) Biochim. Biophys. Acta 766, 492–500.
13 Moreno-Sanchez, R. (1985) J. Biol. Chem. 260, 12554–12560.
14 Mazat, J.-P., Jean-Bart, E., Rigoulet, M. and Guerin, B. (1986) Biochim. Biophys. Acta 849, 7–15.
15 Forman, N.G. and Wilson, D.F. (1983) J. Biol. Chem. 258 (14), 8649–8655.
16 Holian, A., Owen, C.S. and Wilson, D.F. (1977) Arch. Biochem. Biophys. 181, 164–171.
17 Williamson, J.R. and Cooper, R.H. (1980) FEBS Lett. 117, I 73–K85
18 Brown, G.C., Hofner, R.P. and Brand, M.D. (1990) Eur. J. Biochem. 188, 321–325.
19 Brown, G.C., Lakin-Thomas, P.L. and Brand, M.D. (1990) Eur. J. Biochem. 192, 355–362.
20 Hafner, R.P., Brown, G.C. and Brand, M.D. (1990) Eur. J. Biochem. 188, 313–319.
21 Reich, J.G. and Sel'kow, E.E. (1982), in Energy Metabolism of the Cell, A Theoretical Treatise, Academic Press, London.

22 Kunz, W., Bohnensack, R., Böhme, G., Küster, U., Letko, G. and Schönfeld, P. (1981) Arch. Biochem. Biophys. 209, 219–229.
23 Gellerich, F.N., Kunz, W.S. and Bohnensack, R. (1990), FEBS Lett. 274 (1,2), 167–170.
24 Taylor, W.M., Van de Pol, E. and Bygrave, L. (1986) Eur. J. Biochem. 155, 319–322.
25 Kimura, S., Suzaki, T. Kobayashi, S., Abe, K. and Ogata, E. (1984) Biochem. Biophys. Res. Commun. 119 (1), 212–219.
26 Strzelecki, T., Thomas, J.A., Koch, C.D. and LaNoue, K.F. (1984) J. Biol. Chem. 259 (7), 4122–4129.
27 Titheradge, M.A. and Haynes, R.C., (1980) Arch. Biochem. Biophys. 201 (1), 44–55.